Coagulation of an initially monodisperse aerosol

"Smoluchowski constant kernel solution"

Assume $\beta = \dfrac{8kT}{3\mu} = K = \text{const}$

(valid in early stage of monodisperse coagulation in the continuum regime)

$$\frac{dn_k}{dt} = \frac{K}{2}\sum_{i+j=k} n_i n_j - K n_k \sum_{i=1}^{\infty} n_i \cdots (1)$$

$$\sum_{k=1}^{\infty}(1) \rightarrow \frac{dN_\infty}{dt} = \frac{K}{2}\sum_{k=1}^{\infty}\sum_{i+j=k} n_i n_j - K N_\infty{}^2$$

$$\sum_{k=2}^{\infty}\sum_{i+j=k} n_i n_j = \sum_{i=1}^{\infty} n_i \sum_{j=1}^{\infty} n_j$$

k=1, i+j=1 $\rightarrow$ impossible. Therefore, Eq(1) is valid for k $\geq$ 2

For k=1, $\dfrac{dn_1}{dt} = -Kn_1 \sum_{i=1}^{\infty} n_i$

$$\therefore \frac{dN_\infty}{dt} = -\frac{K}{2} N_\infty{}^2$$

$$\therefore N_\infty(t) = \frac{N_\infty(0)}{1 + \frac{KN_\infty(0)}{2} t} = \frac{N_\infty(0)}{1 + t/\Im_c}, \quad \Im_c = \frac{2}{KN_\infty(0)}$$

$\Im_c$: characteristic time for coagulation

large times $t >> \Im_c$ $\quad N_\infty(t) = \dfrac{2}{Kt}$

independent of initial concentration

$\Im_c$ becomes larger for smaller $N_\infty(0) \rightarrow$ to freeze particle size distribution,

dilute the aerosol rapidly

Mass concentration remains constant

$$C = N_\infty(0)\frac{\pi}{6}\rho_p {d_0}^3 = N(t)\frac{\pi}{6}\rho_p d(t)^3$$

$d(t)$:average diameter $d(t)$

$$\frac{d(t)}{d_0} = \left(\frac{N_\infty(0)}{N(t)}\right)^{1/3} \rightarrow \text{diameter of average mass}$$

$$\frac{dn_1}{dt} = -Kn_1N_\infty = -Kn_1\frac{N_\infty(0)}{1+ t/\Im_c}$$

$$\ln\frac{n_1(t)}{N_\infty(0)} = -K\Im_c N_\infty(0)\ln\left(1+\frac{t}{\Im_c}\right) \quad \therefore n_1(t) = \frac{N_\infty(0)}{\left(1+ t/\Im_c\right)^2}$$

$N_\infty(0)$ (#/cm3)	$\Im_c$	time for particle size to double
10^{14}	$20\mu s$	$140\mu s$
10^{10}	0.2sec	1.4sec
10^{4}	55hr	16days
10^{2}	231days	4year

$$\frac{dn_2}{dt} = \frac{K}{2}\sum_{i+j=2} n_i n_i - Kn_2 N_\infty = \frac{K}{2} n_1^{\ 2} - Kn_2 N_\infty$$

$$\therefore n_2 = \frac{N_\infty(0)\ {}^{t}\!/_{\Im_c}}{\left(1 + {}^{t}\!/_{\Im_c}\right)^3}$$

In general,

$$n_k = \frac{N_\infty(0)\left({}^{t}\!/_{\Im_c}\right)^{k-1}}{\left(1 + {}^{t}\!/_{\Im_c}\right)^{k+1}} \qquad t >> \Im_c \qquad n_k(t) = N_\infty(0)\left({}^{t}\!/_{\Im_c}\right)^{-2} \sim \frac{1}{t^2}$$

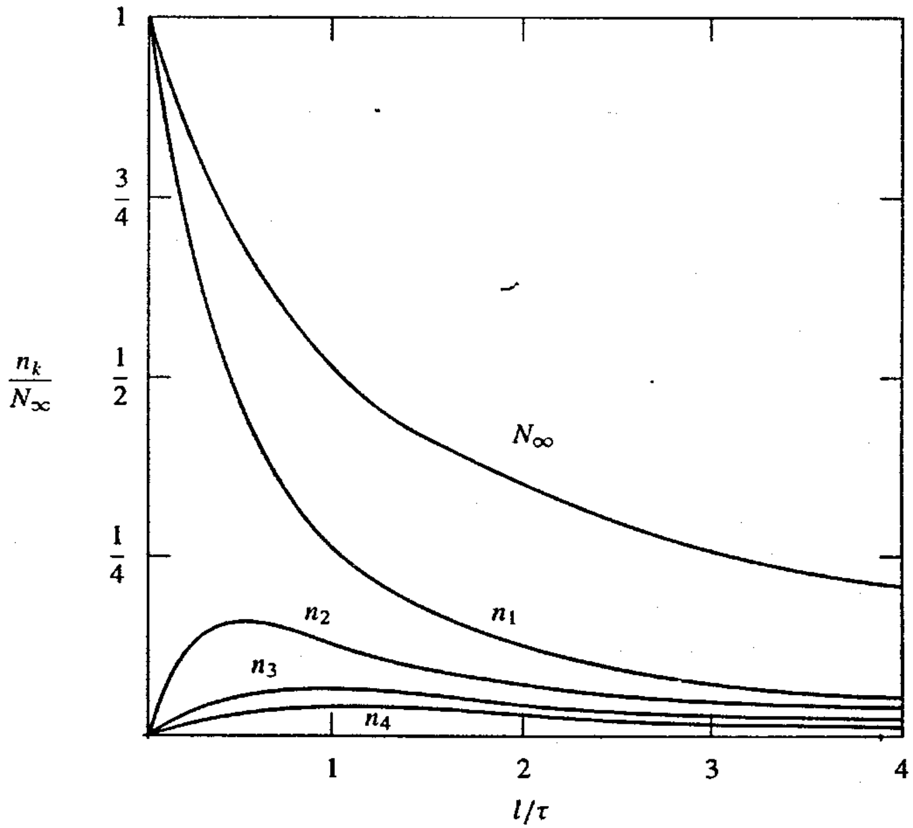

Fig.14 The Variations in N_∞, n_1, n_2… with time for an initially monodisperse aerosol. The total number concentration, N_∞, and the concentration of n_1 both decrease monotonically with increasing time. The concentration of n_2 …pass through a maximum. (After Smoluchowski, 1917)

Effect of particle force fields

#/m2 sec $J = -D\dfrac{\partial n}{\partial r} + cn \rightarrow$ drift velocity due to inter particle force

c=BF

$$F = -\frac{d\Phi_r}{dr} \qquad \Phi_r = \text{Potential energy}$$

$$D = \frac{kT}{f} = kTB \qquad B = \frac{1}{f}:\text{particle mobility}$$

Steady State

$$4\pi r^2 J = \text{const}$$

$$= -D4\pi r^2 \frac{\partial n}{\partial r} + (4\pi r^2)\frac{D}{kT}\left(-\frac{d\Phi_{(r)}}{dr}\right) n = \text{const} = \mathrm{G}$$

$$\therefore n = n_\infty \exp\left(-\frac{\Phi_{(r)}}{kT}\right) + \frac{G\exp\left(-\frac{\Phi_{(r)}}{kT}\right)}{4\pi D} \times \int_\infty^r \frac{\exp\left(\frac{\Phi_{(r)}}{k}\right)}{x^2} dx$$

at $r = a_i + a_j$, $n = 0$ condition

$$G = \frac{4\pi D n_\infty (a_i + a_j)}{W}$$ W: correction factor

$$W = (a_i + a_j)\int_{a_i + a_j}^{\infty} \left[\exp^{\left(\Phi(x) / kT \right)} \Big/ x^2 \right] dx$$

(1) Van der Waals force due to fluctuating dipoles :

attractive force two spherical particles of radii a_i and a_j

$$\Phi = -\frac{\pi^2 Q}{6}\left[\frac{2a_i a_j}{r^2 - \left(a_i + a_j\right)^2} + \frac{2a_i a_j}{r^2 - \left(a_i - a_j\right)^2} + \ln \frac{r^2 - \left(a_i + a_j\right)^2}{r^2 - \left(a_i - a_j\right)^2} \right]$$

$Q = \dfrac{4\varepsilon\sigma^6}{{v_m}^2}$: Hamaker Constant, v_m : molecular volume

Lennard - Jones force constants ε, σ

Table 7. P.198, Friedlander

TABLE 7.1
Hamaker Constants for Two Identical Substances Interacting Across Vacuum (or Gas at Low Pressure) (from Israelachvili, 1992, p. 186)

Substance	A (10^{-20} J)
Water	3.7
Cyclohexane	5.2
Benzene	5.0
Polystyrene	6.5
Fused Quartz	6.3
Alumina (Al_2O_3)	14
Iron Oxide (Fe_2O_3)	21
Rutile (TiO_2)	43
Metals (Au, Ag, Cu)	25–40

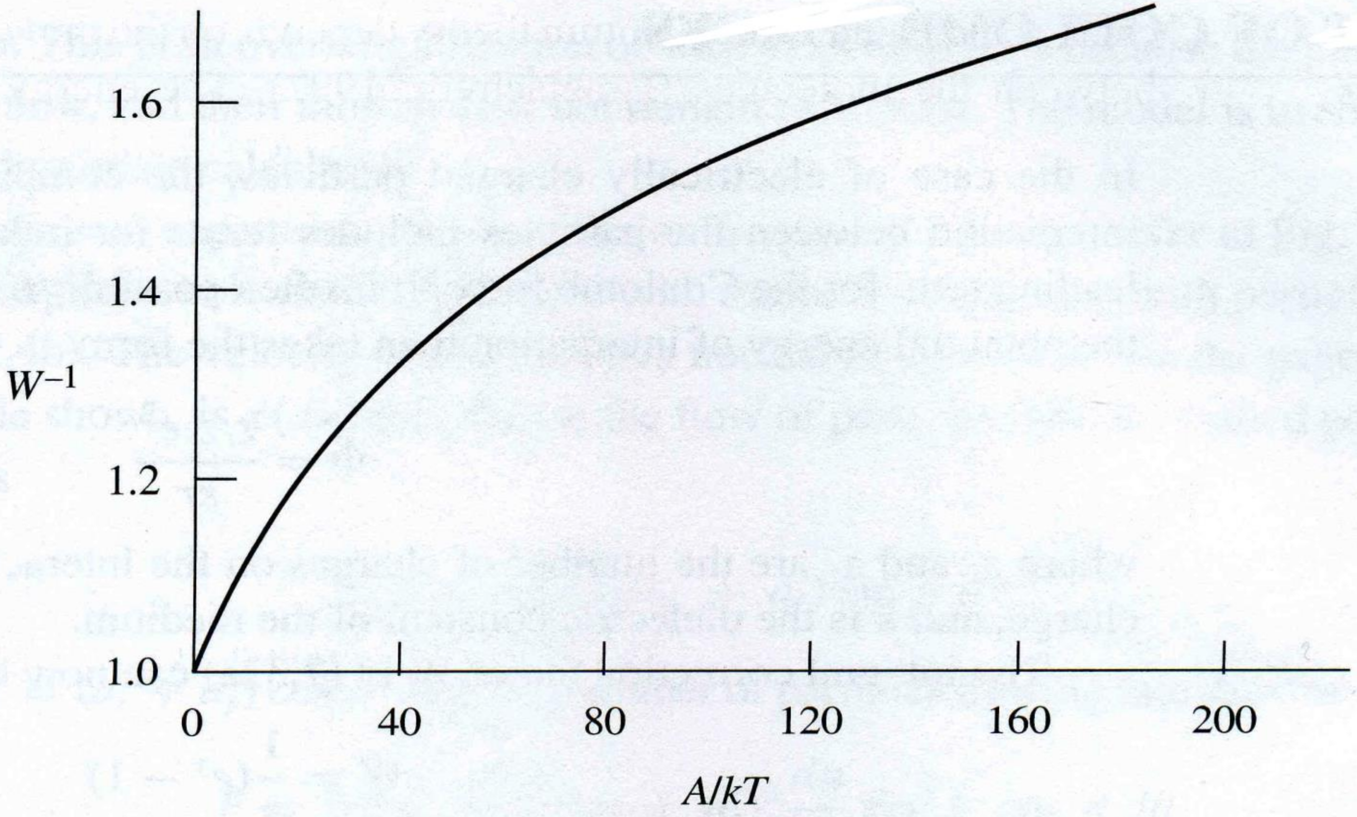

Figure 7.3 Increase in rate of collision of particles of equal diameter resulting from the action of van der Waals forces (Tikhomirov et al., 1942).

(2) Coulomb force

$$\Phi = \frac{Z_i Z_j e^2}{\varepsilon r}$$

$Z_i Z_j$: number of charges of i and j particles

ε : dielectric constant of the medium

$$W = \frac{1}{y}(e^y - 1)$$

$$y = \frac{Z_i Z_j e^2}{\varepsilon k T (a_i + a_j)}$$

for uncharged particles, $y = 0$ $W = 1$

$W \approx 1+\dfrac{y}{2}$ for small y

If particles have opposite charges,

y is negative $1>W>0$

$\therefore$ enhanced collision

If particles are of like sign, $y>0$, $W>1$:

collision rate is smaller than for uncharged particles

For bipolar aerosols, $|y|<\dfrac{1}{2} \rightarrow$ the effect should be a small increase in coagulation

attractive forces compensate the

decrease caused by repulsion

but $|y|>>1$ bipolar aerosols $\rightarrow$ large increase in coagulation

The large increase in coagulation resulting from attractive forces strongly outweighs the decrease caused by repulsion (Friedlander, p200)

Collision frequency function for laminar shear : Simplified analysis : Smoluchowski

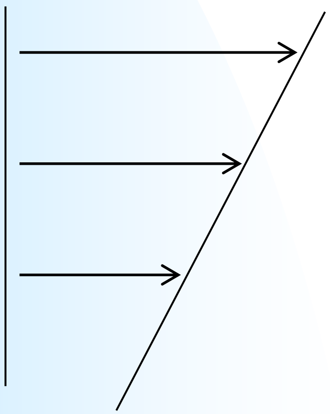

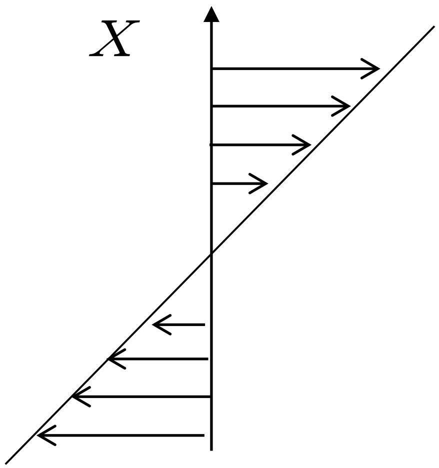

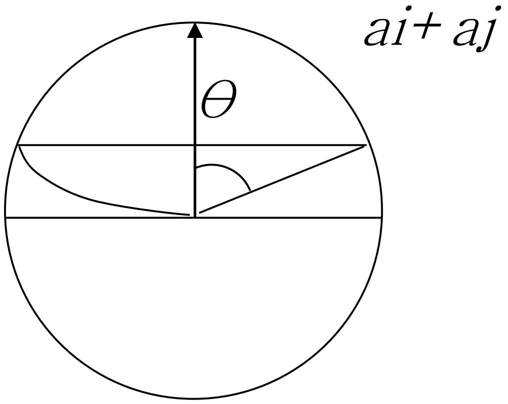

dF : particle flow into the shaded portion of the strip dx

$$dF = n_j x \frac{du}{dx}(a_i + a_j)\sin\theta dx$$

$$x = (a_i + a_j)\cos\theta$$

$$F = 4n_j \int_0^{\frac{\pi}{2}} (a_i + a_j)^3 \frac{du}{dx} \sin^2\theta \cos\theta \, d\theta$$

$$= \frac{4}{3}(a_i + a_j)^3 \frac{du}{dx} n_j$$

$$\therefore \beta(v_i, v_j) = \frac{4}{3}(a_i + a_j)^3 \frac{du}{dx}$$

For equal size $\beta = \frac{4}{3} d_p{}^3 \frac{du}{dx}$ (Brownian $\beta = \frac{8kT}{3\mu}$)

$$\beta_{LS} \big/ \beta_B = \frac{1}{2} \frac{\frac{du}{dx}}{k\,T} \mu d_p{}^3, i.e.,$$ β_{LS} becomes more important for larger d_p

for fixed $du \big/ dx$

For nearly same sized particles

$$\frac{dn_k}{dt} = \frac{1}{2} \sum_{i+j=k} \frac{32}{3} a^3 \frac{du}{dx} n_i n_j - \sum_{i=1}^{\infty} \frac{32}{3} a^3 \frac{du}{dx} n_i n_k$$

$$\frac{dN_\infty}{dt} = -\frac{16}{3} \frac{du}{dx} a^3 N_\infty{}^2 : a(t), N_\infty(t)$$

$$\frac{4}{3}\pi a^3 N_\infty = V = \text{const}$$

$$\frac{dN_\infty}{dt} = -\frac{4V}{\pi}\frac{du}{dx}N_\infty \propto N_\infty$$

$$\ln\frac{N_\infty(0)}{N_\infty} = \frac{4V}{\pi}\frac{du}{dx}t$$

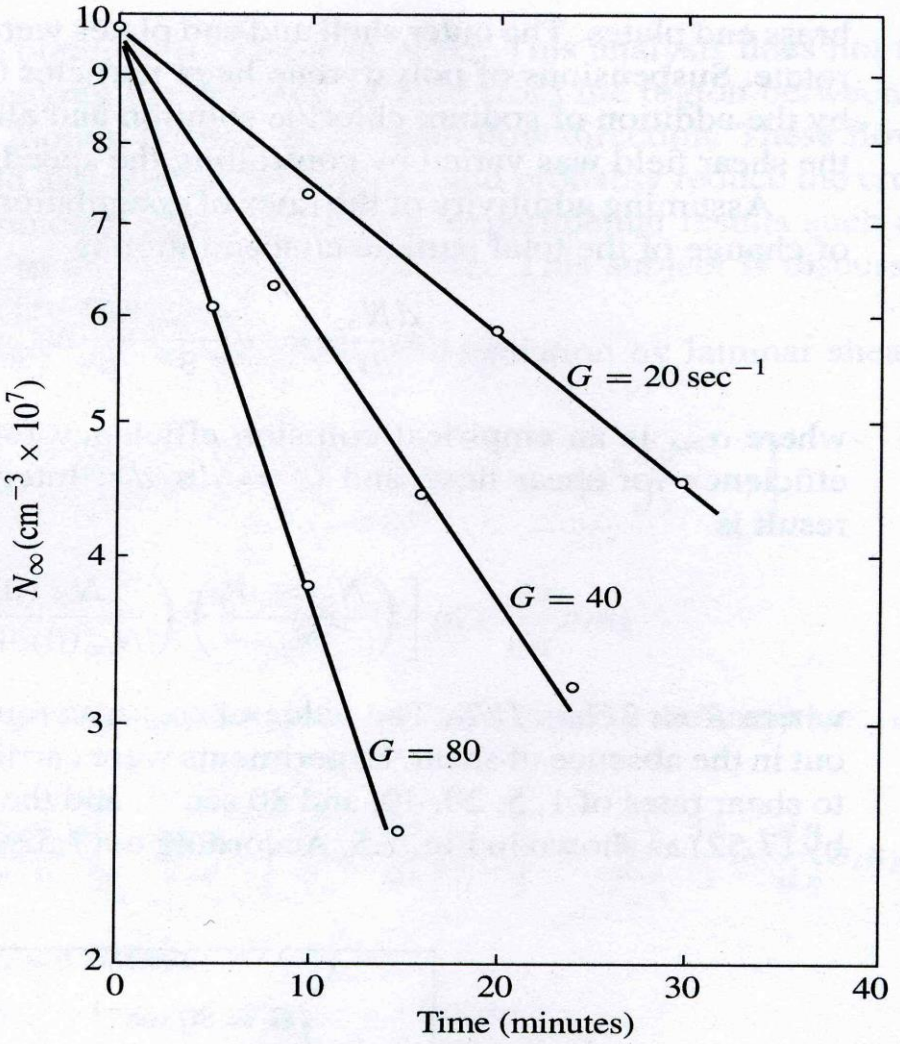

Figure 7.6 When shear coagulation dominates, a plot of log N_∞ versus t should give a straight line. This was confirmed experimentally at the higher shear rates with a monodisperse hydrosol (Swift and Friedlander, 1964).

Other Collision Mechanism

Turbulent shear

$$\beta = \left(\frac{\pi \varepsilon_k}{120 v} \right)^{1/2} \left(d_{p1} + d_{p2} \right)^3$$

$\leftarrow$ Saffman and Turner(1956),

On the Collision of drops in Turbulent clouds,

JFM, vol.1, pp.16-30

$$\left(\frac{\varepsilon_k}{v} \right)^{1/2} \leftrightarrow \frac{du}{dx} \text{ lamina shear}$$

turbulent shear

ε_k :energy dissipation by turbulence

(cm2/sec3) : rate of dissipation of kinetic energy per unit mass

$$\varepsilon_k = \frac{4}{d}\left(\frac{f}{2}\right)^{3/2} U^3 \quad \text{for a pipe flow}$$

f: Fanning friction factor

$$\Im_w = f \cdot \frac{1}{2}\rho U^2 \qquad \text{:Fanning friction factor}$$

$$\Delta p = 4f\,\frac{L}{D_h}\frac{1}{2}\rho U^2 \quad \text{:Darcy friction } \rightarrow \text{ Moody chart}$$

Differential sedimentation

$$\beta = \gamma \cdot \pi (a_i + a_j)^2 (v_i - v_j) \quad \gamma : \text{capture efficiency}$$

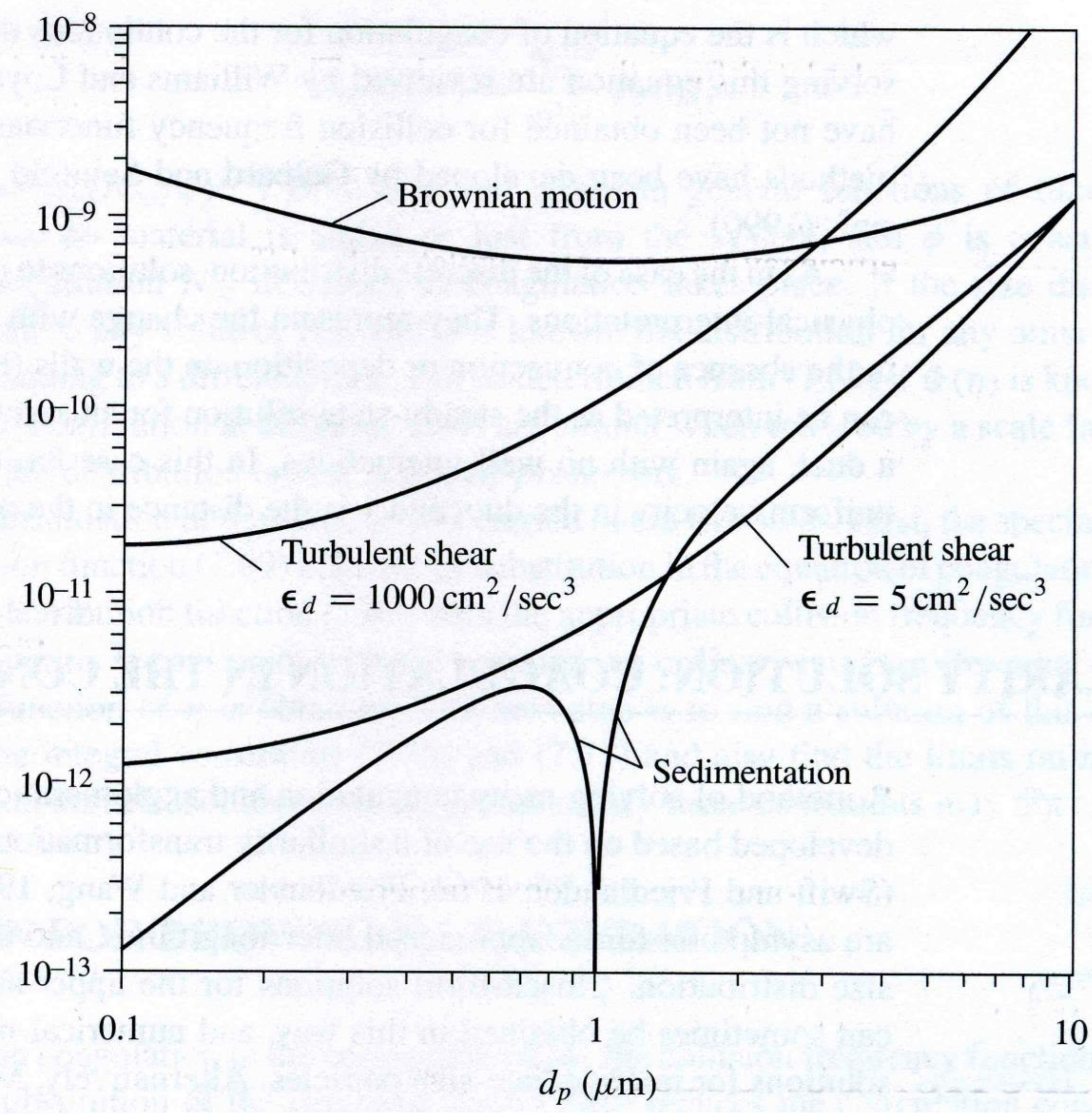
10^{-8}
10^{-9}
10^{-10}
10^{-11}
10^{-12}
10^{-13}
β (cm^3/sec)
Brownian motion
Turbulent shear
$\epsilon_d = 1000$ cm^2/sec^3
Turbulent shear
$\epsilon_d = 5$ cm^2/sec^3
Sedimentation
0.1
1
10
d_p (μm)

Figure 7.7 Comparison of coagulation mechanisms for particles of 1-μm diameter interacting with particles of diameter between 0.1 and 10 μm. Coagulation by shear based on $\epsilon_d = 5$ and 1000 cm^2/sec^3. Differential sedimentation curves were obtained by an approximate calculation assuming Stokes flow around the larger of the falling spheres (Friedlander, 1964). $\epsilon_d = 5\ \text{cm}^2/\text{sec}^3$ corresponds to the open atmosphere at a height of about 100 m (Lumley and Panofsky, 1964). At a height of 1 m, $\epsilon_d \approx 1000\ \text{cm}^2/\text{sec}^3$ and shear becomes the dominant mechanism of coagulation for larger particles. For the core region of a turbulent pipe flow, the energy dissipation (based on Laufer, 1954) is given by

$$\epsilon_d = \frac{4}{d}\left(\frac{f}{2}\right)^{3/2} U^3$$

where f is the Fanning friction factor, d is the pipe diameter, and U is the gas velocity. For a smooth pipe, 10 cm in diameter, with air at 20°C and a Reynolds number of 50,000, $\epsilon_d \approx 2 \times 10^4\ \text{cm}^2/\text{sec}^3$.

Particle dynamics for continuous distribution function

$$\frac{dn_k}{dt} = \frac{1}{2}\sum_{i+j=k} N_{ij} - \sum_{i=1}^{\infty} N_{ik}$$

$$= \frac{1}{2}\sum_{i+j=k} \beta(v_i, v_j) n_i n_j - n_k \sum_{i=1}^{\infty} \beta(v_i, v_k) n_i$$

$$N_{v\tilde{v}} = \beta(v, \tilde{v}) n(v) n(\tilde{v}) dv\, d\tilde{v}$$

$$\frac{\partial(ndv)}{\partial t} = \frac{1}{2}\left[\int_0^v \beta(\tilde{v}, v-\tilde{v}) n(\tilde{v}) n(v-\tilde{v}) d\tilde{v}\right] dv$$

$$-\left[\int_0^\infty \beta(v, \tilde{v}) n(\tilde{v}) n(v) d\tilde{v})\right] dv$$

Self Preserving Distribution

-Similarity solution exists after long time passes (pure coagulation)

-They are independent of initial size distribution.

$$\frac{ndv}{N_\infty} = \psi\left(\frac{v}{\bar{v}}\right) d\left(\frac{v}{\bar{v}}\right) \qquad \bar{v} = \frac{V}{N_\infty}$$

- Fraction of particles in a given size range is a function only of particle volume normalized by the average particle volume

$$n(v,t) = \frac{N_\infty{}^2}{V}\psi(\eta) \qquad \eta = \frac{v}{\bar{v}} = \frac{N_\infty v}{V}$$

$$N_\infty = \int_0^\infty n dv$$

$$V = \int_0^\infty nv\, dv$$

In terms of particle radius a,

$$v = \frac{4}{3}\pi a^3 \qquad n_a(a)da = n(v)dv$$

$$\therefore n_a(a) = 4\pi a^2 n(v)$$

$$\eta = \frac{N_\infty v}{V} = \frac{N_\infty}{V}\frac{4}{3}\pi a^3 \propto \left\{\left(\frac{N_\infty}{V}\right)^{1/3} a\right\}^3 \qquad \therefore \eta_a = a\left(\frac{N_\infty}{V}\right)^{1/3}$$

$$\frac{n_a(a)}{4\pi a^2} = \frac{N_\infty{}^2}{V}\psi_a(\eta_a) \qquad n_a(a) = 4\pi a^2 \frac{N_\infty{}^2}{V}\psi_a(\eta_a)$$

since $$4\pi a^2 \frac{N_\infty{}^2}{V} = 4\pi \eta_a{}^2 \frac{N_\infty{}^{4/3}}{V^{1/3}}$$

$$\rightarrow \quad \therefore n_a(a,t) = \frac{N_\infty{}^{4/3}}{V^{1/3}}\psi_a(\eta_a)$$

Friedlander, p. 211

$$n_d(d_p, t) = \frac{N_\infty^{4/3}}{\phi^{1/3}} \psi_d(\eta_d) \tag{7.72}$$

where $\eta_d = d_p(N_\infty/\phi)^{1/3}$. Both N_∞ and ϕ are in general functions of time. In the simplest case, no material is added or lost from the system, and ϕ is constant. The number concentration N_∞ decreases as coagulation takes place. If the size distribution corresponding to any value of N_∞ and ϕ is known, the distribution for any other value of N_∞ corresponding to a different time, can be determined from (7.69) if $\psi(\eta)$ is known. The shapes of the distribution at different times are similar when reduced by a scale factor. For this reason, the distribution is said to be *self-preserving*.

The determination of the form of ψ is carried out in two steps. First, the special form of the distribution function (7.69) is tested by substitution in the equation of coagulation for the continuous distribution function (7.67) with the appropriate collision frequency function. If the transformation is consistent with the equation, an ordinary integrodifferential equation for ψ as a function of η is obtained. The next step is to find a solution of this equation subject to the integral constraints (7.70) and (7.71) and also find the limits on $n(v)$. For some collision kernels, solutions for $\psi(\eta)$ that satisfy these constraints may not exist.

For Brownian coagulation in the continuum range, the collision frequency function is given by (7.16). Substitution of the similarity form (7.69) reduces the coagulation equation for the continuous distribution (7.67) with (7.16) to the following form:

$$\frac{1}{N_\infty^2}\frac{dN_\infty}{dt}\left[2\psi+\eta\frac{d\psi}{d\eta}\right]$$
$$=\frac{kT}{3\mu}\int_0^\eta \psi(\tilde{\eta})\psi(\eta-\tilde{\eta})\left[\tilde{\eta}^{1/3}+(\eta-\tilde{\eta})^{1/3}\right]\left[\frac{1}{\tilde{\eta}^{1/3}}+\frac{1}{(\eta-\tilde{\eta})^{1/3}}\right]d\tilde{\eta}$$
$$-\frac{2kT}{3\mu}\psi(\eta)\int_0^\infty \psi(\tilde{\eta})\left[\eta^{1/3}+\tilde{\eta}^{1/3}\right]\left[\frac{1}{\eta^{1/3}}+\frac{1}{\tilde{\eta}^{1/3}}\right]d\tilde{\eta} \tag{7.73}$$

The change in the total number concentration with time is found by integrating over all collisions:

$$\frac{dN_\infty}{dt}=-\frac{1}{2}\int_0^\infty\int_0^\infty \beta(v,\tilde{v})n(v)n(\tilde{v})\,dv\,d\tilde{v} \tag{7.74}$$

The factor 1/2 is introduced because the double integral counts each collision twice. By substituting (7.69) and (7.16) in (7.74), we obtain

$$\frac{dN_\infty}{dt}=-\frac{2kT}{3\mu}(1+ab)N_\infty^2 \tag{7.75}$$

where

$$a=\int_0^\infty \eta^{1/3}\psi\,d\eta \tag{7.75a}$$

and

$$b = \int_0^\infty \eta^{-1/3} \psi \, d\eta \tag{7.75b}$$

Equation (7.76) is of the same form as (7.21) for the decay of the total number concentration in a monodisperse system. However, the constant has a somewhat different value. Substituting (7.75) in (7.73) and consolidating terms, the result is

$$(1 + ab)\eta \frac{d\psi}{d\eta} + \left(2ab - b\eta^{1/3} - a\eta^{-1/3}\right)\psi + \int_0^\eta \psi(\eta - \tilde{\eta})\psi(\tilde{\eta}) \left[1 + \left(\frac{\eta - \tilde{\eta}}{\tilde{\eta}}\right)^{1/3}\right] d\tilde{\eta} = 0 \tag{7.76}$$

which is an ordinary integrodifferential equation for ψ with η the independent variable. Hence the similarity transformation (7.69) represents a possible particular solution to the coagulation equation with the Brownian motion coagulation mechanism.

It is still necessary to show that a solution can be found to the transformed equation (7.76) with the integral constraints, (7.70) and (7.71). Analytical solutions to (7.76) can be found for the upper and lower ends of the distribution by making suitable approximations (Friedlander and Wang, 1966). The complete distribution can be obtained numerically by matching the distributions for the upper and lower ends, subject to the integral constraints that follow from (7.70) and (7.71):

$$\int_0^\infty \psi \, d\eta = 1 \tag{7.76a}$$

and

$$\int_0^\infty \eta\psi \, d\eta = 1 \tag{7.76b}$$

The results of the numerical calculation are shown in Fig. 7.8, where they are compared with numerical calculations carried out for the discrete spectrum starting with an initially monodisperse system. There is good agreement between the two methods of calculation. Other calculations indicate that the similarity form is an asymptotic solution independent of the initial distributions so far studied. The values of a and b were found to be 0.9046 and 1.248, respectively. By (7.75) this corresponds to a 6.5% increase in the coagulation constant compared with the value for a monodisperse aerosol (7.21). The results of more recent calculations using a discrete sectional method are shown in Table 7.2.

To predict the size distribution of a uniform aerosol coagulating in a chamber without deposition on the walls, the following procedure can be adopted: The volumetric concentration of aerosol is assumed constant and equal to its (known) initial value. The change in the number concentration with time is calculated from (7.75). The size distribution at any time can then be determined for each value of $v = \phi\eta/N_\infty$ from the relation $n = (N_\infty^2/\phi)\psi(\eta)$, using the tabulated values. The calculation is carried out for a range of values of η.

SIMILARITY SOLUTION: COAGULATION IN THE FREE MOLECULE REGION

Is it possible to make the similarity transformation (7.62) for other collision mechanisms? In general, when the collision frequency $\beta(v, \tilde{v})$ is a homogeneous function of particle volume, the transformation to an ordinary integrodifferential equation can be made. The function $\beta(v, \tilde{v})$ is said to be *homogeneous* of degree λ if $\beta(\alpha v, \alpha \tilde{v}) = \alpha^{\lambda} \beta(v, \tilde{v})$. However, even though the transformation is possible, a solution to the transformed equation may not exist that satisfies the boundary conditions and integral constraints.

When the particles are much smaller than the mean free path, the collision frequency function is given by (7.17)

$$\beta(v, \tilde{v}) = \left(\frac{3}{4\pi}\right)^{1/6} \left(\frac{6kT}{\rho_p}\right)^{1/2} \left[\frac{1}{v} + \frac{1}{\tilde{v}}\right]^{1/2} \left(v^{1/3} + \tilde{v}^{1/3}\right)^2$$

which is a homogeneous function of order 1/6 in particle volume. The similarity transformation can be made and a solution can be found to the transformed equation in much the same way as in the previous sections (Lai et al., 1972). Values of the dimensionless size distribution function $\psi(\eta)$ for the free molecule and continuum regimes are also given in Table 7.2. For the free molecule regime, the change in the total number of particles with time is

$$\frac{dN_\infty}{dt} = -\frac{\alpha}{2} \left(\frac{3}{4\pi}\right)^{1/6} \left(\frac{6kT}{\rho_p}\right)^{1/2} \phi^{1/6} N_\infty^{11/6} \tag{7.77}$$

The constant α is an integral function of ψ and is found to be about 6.67 by numerical analysis.

TABLE 7.2
Values of the Self-Preserving Size Distribution for the Continuum (ψ_c) and Free Molecule (ψ_f) Regimes Calculated by a Discrete Sectional Method (Vemury and Pratsinis, 1995)

η	ψ_f	ψ_c
0.006	0.0408	0.1218
0.007	0.0632	0.1581
0.008	0.0891	0.1933
0.009	0.1176	0.2271
0.010	0.1479	0.2592
0.015	0.3079	0.2895
0.020	0.4560	0.4170
0.025	0.5809	0.5124
0.030	0.6830	0.5852
0.035	0.7654	0.6418
0.040	0.8315	0.6868
0.045	0.8846	0.7230
0.050	0.9271	0.7525
0.060	0.9880	0.7766
0.070	1.0261	0.8132
0.080	1.0486	0.8384
0.090	1.0605	0.8559
0.1	1.0649	0.8678
0.2	0.9668	0.8755
0.3	0.8351	0.8563
0.4	0.7232	0.7883
0.5	0.6309	0.7156
0.6	0.5542	0.6466
0.7	0.4895	0.5830
0.8	0.4344	0.5252
0.9	0.3871	0.4730
1.0	0.3459	0.4259
1.5	0.2041	0.3834
2.0	0.1247	0.2271
2.5	0.0777	0.1348

TABLE 7.2
Continued

continued

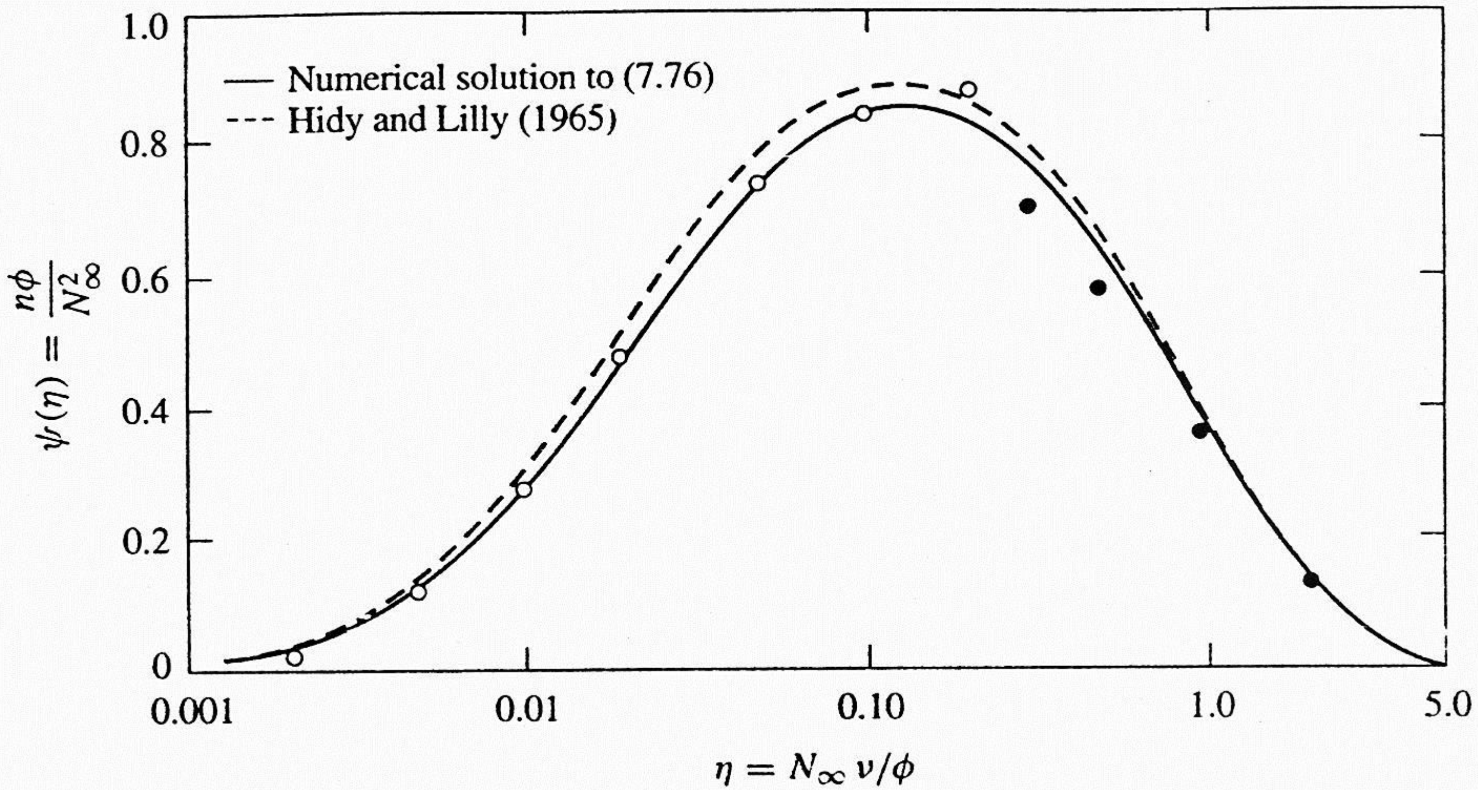

Figure 7.8 Self-preserving particle size distribution for Brownian coagulation. The form is approximately lognormal. The result obtained by solution of the ordinary integrodifferential equation for the continuous spectrum is compared with the limiting solution of Hidy and Lilly (1965) for the discrete spectrum, calculated from the discrete form of the coagulation equation. Shown also are points calculated from analytical solutions for the lower and upper ends of the distribution (Friedlander and Wang, 1966).

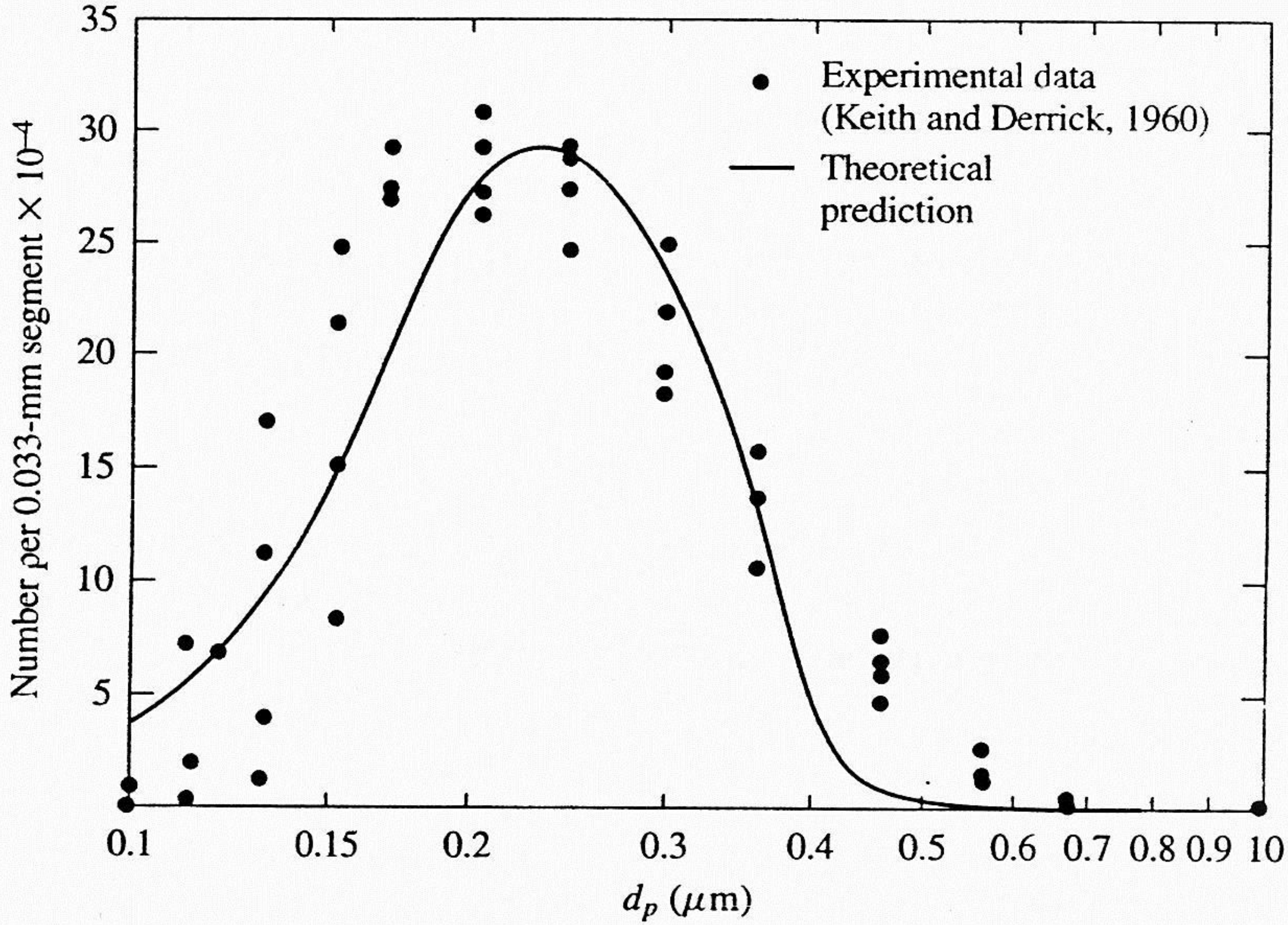

Figure 7.9 Comparison of experimental size distribution data for tobacco smoke with prediction based on self-preserving size spectrum theory. $\phi = 1.11 \times 10^{-7}$, $N_\infty = 1.59 \times 10^7$ cm^{-3}. The peak in the number distribution measured in this way occurs at $d_p \approx 0.2$ μm (Friedlander and Hidy, 1969).

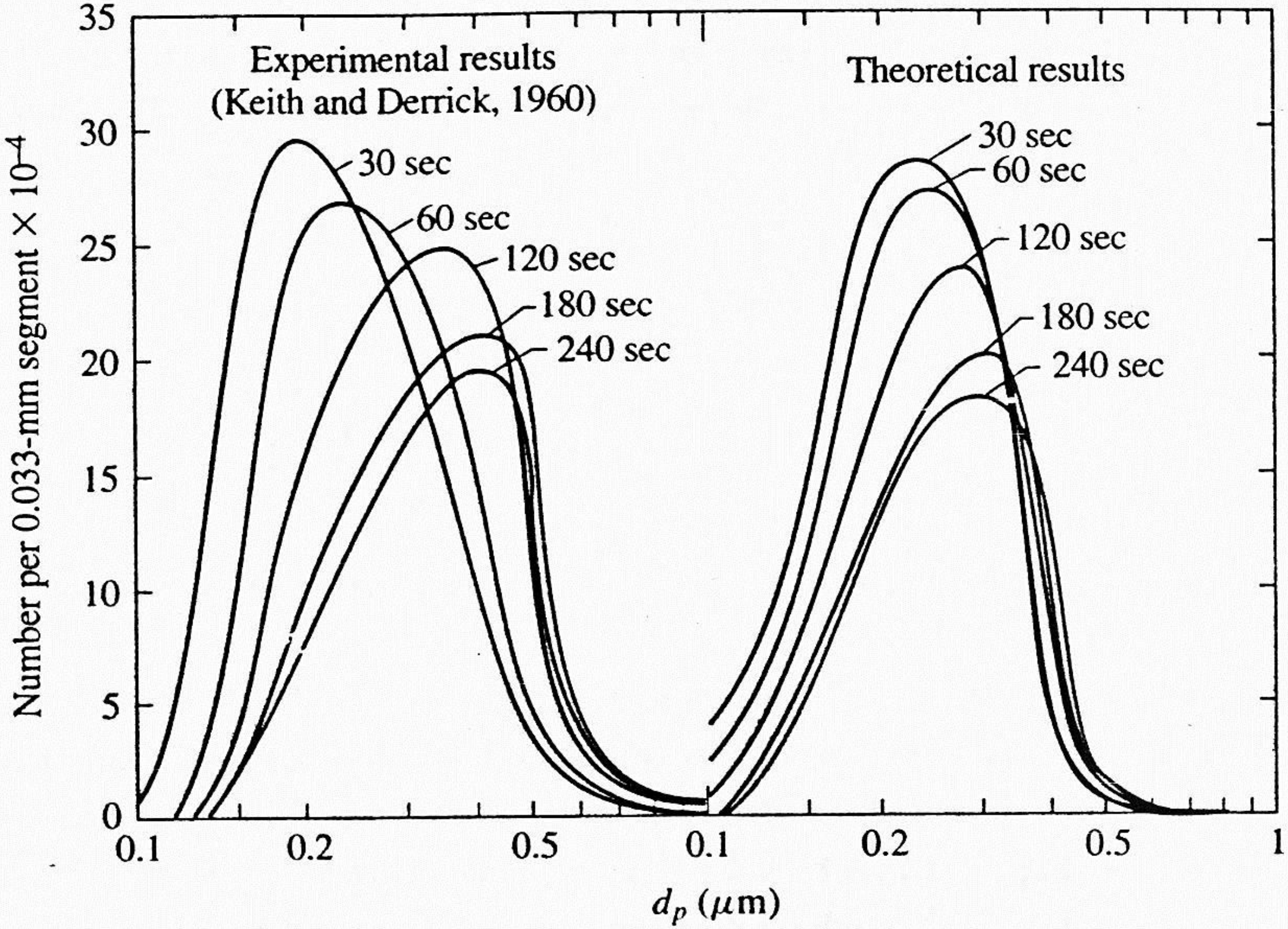

Figure 7.10 Experiment and theory compared for an aging tobacco smoke aerosol. Calculation based on $\phi = 1.11 \times 10^{-7}$ and experimental values of N_∞ (Friedlander and Hidy, 1969).

Husar (1971) studied the coagulation of ultrafine particles produced by a propane torch aerosol in a 90-m^3 polyethylene bag. The size distribution was measured as a function of time with an electrical mobility analyzer. The results of the experiments are shown in Fig. 7.11 in which the size distribution is plotted as a function of particle diameter and in Fig. 7.12 in which ψ is shown as a function of η both based on particle radius. Numerical calculations were carried out by a Monte Carlo method, and the results of the calculation are also shown in Fig. 7.12. The agreement between experiment and the numerical calculations is quite satisfactory.

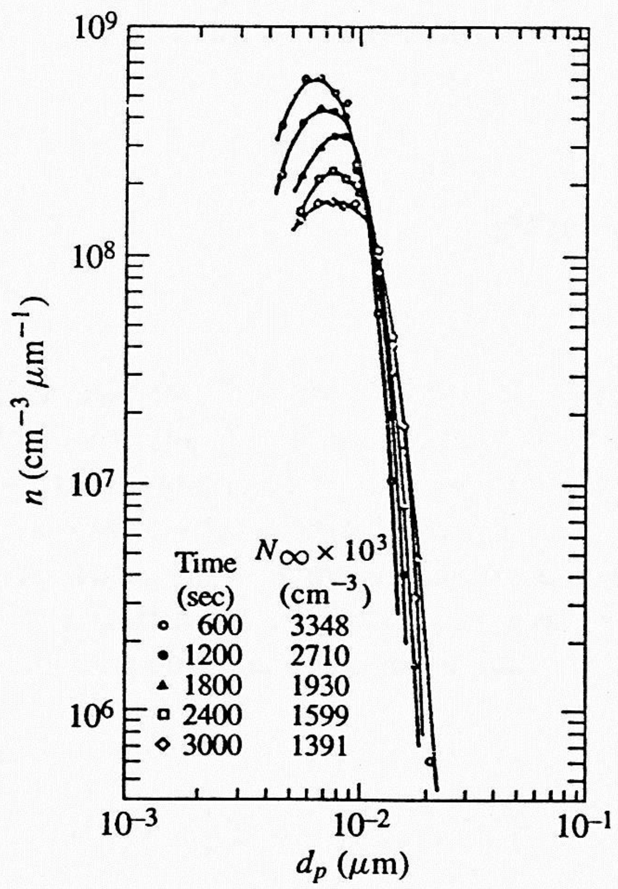

Figure 7.11 Coagulation of aerosol particles much smaller than the mean free path. Size distributions measured with the electrical mobility analyzer (Husar, 1971).

rsity
e Control

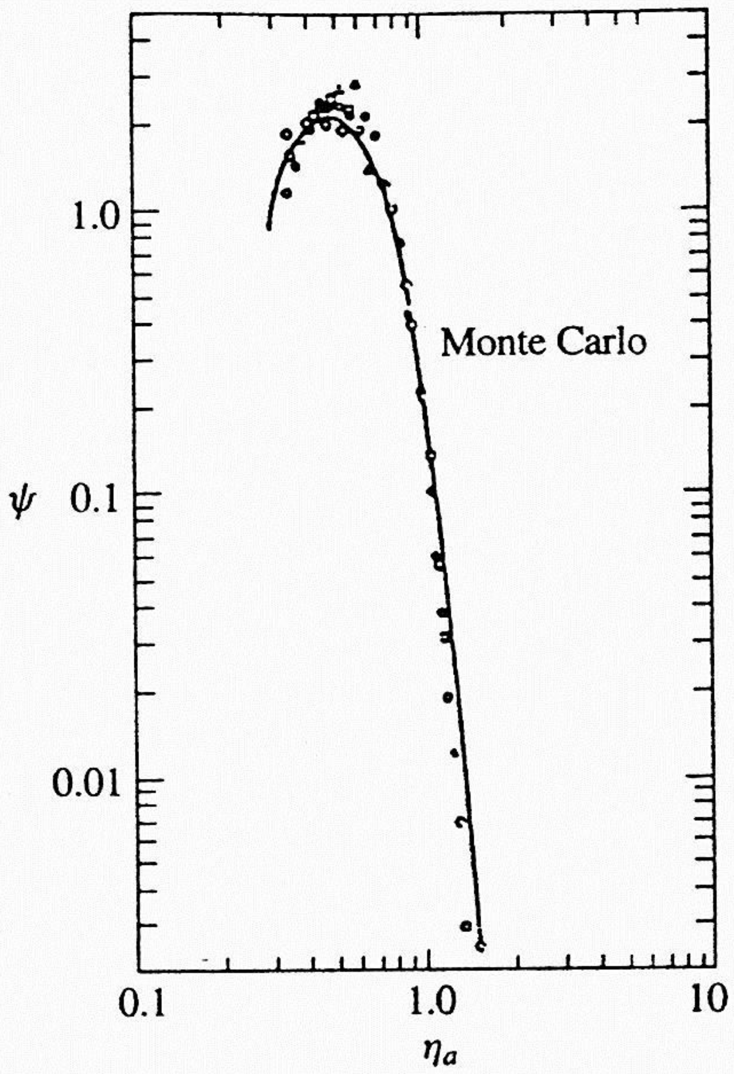

Figure 7.12 Size distribution data of Fig. 7.11 for coagulation of small particles plotted in the coordinates of the similarity theory. Shown also is the result of a Monte Carlo calculation for the discrete spectrum (Husar, 1971).